

Performance Evaluation of Power in GSM BTS in Nigeria Using PV Solar System

Goshwe, N. Y., Kureve, T. D., Okeleke, A.

Department of Electrical & Electronics Engineering, University of Agriculture, Makurdi

Abstract

In a typical Global System of Mobile (GSM) communications, Base Transceiver Station (BTS); the network security and availability with respect to transmission of network signals is a function of power availability on site. This research project is directly aimed at achieving power availability with minimum overhead expenses in respect of fuel consumption on site's generators. A solar panel is employed as the main supply of power; energy from the sun is converted into dc form through the use of converters while a filter circuit is designed at the power supply unit to give an output with low harmonics. The converter circuits are arranged in forward and reverse modes such that when the solar panel is fully insolated (charging mode) the forward mode operates, while the reverse mode operates when the circuit is discharging. A buck-boost converter is employed to step-up or down the voltage output needed at the different stages. An isolator circuit is employed in this design to isolate the low voltage path (dc path) from the high voltage path (ac circuit). Simulations of the various circuits in this design were carried out using Matlab Simulink to clearly describe the waveforms expected at each output of the functional blocks.

Keywords: Transceiver Station (BTS), Global System of Mobile (GSM), Static converter efficiency, Solar Photovoltaic(PV) energy, Inverter.

I. INTRODUCTION

Grid power supply is a major concern in Nigeria and has affected GSM telecom operations in terms of costs and reliability. More than half of the sites are off-grid and usually powered by diesel generators with huge operating expenses. The remaining grid-connected sites suffer due to the poor quality of power supply and frequent outages lasting long hours. This has led to a heavy dependence on diesel generators for the grid-connected sites as well [11].

In addition to the poor grid power supply, Nigerian telecom operators face operation challenges. Site security, for example, is a major issue as there have been several cases of damage to GSM BTS site assets across the country. This risk has hindered GSM service providers from investing in green power alternatives for their network. Thefts of equipment and fuel pilferage have affected the overhead operating costs of BTS sites [11].

Also, initiatives reducing the diesel consumption have been conflicting with O&M partners' interests, thus hampering the successful implementation of these alternatives. The lack of support from the government in providing policy guidelines and security to telecom infrastructure adds to the operational complexity and costs of running a telecom network in Nigeria [11]. These factors go a long way in affecting the optimal network operation and quality of GSM service being offered presently in Nigeria.

1.1 Growth context

While the coverage of mobile network in Nigeria has reached more than 85% of the country's population, mobile penetration is still low, with around 65% of the population using mobile services. The remaining 15% of the uncovered population (approx.. 25 million) presents infrastructure and geographical challenges, hindering the expansion of mobile telecom services coverage.

The scattered and remote nature of these communities also makes it difficult to justify the huge investments by GSM operators aimed at extending their coverage. The government and regulatory support has not been up to the mark in catalyzing the implementation of rural telephony to extend coverage of telecom services to the remote rural communities [11].

1.2 Alternative power choices and their market fit for GSM telecommunication in Nigeria

The choice of alternative power technology in the telecom industry depends on its resource availability, technology supply, commercial viability and market acceptance. The qualification of various alternative power choices suitable for telecom applications including solar, wind, biomass, fuel cell and Pico-hydro, is analyzed below:

1.2.1 Solar

Solar energy is one of the most ubiquitously available sources of clean energy and the most suitable for distributed power generation, bringing power generation to where it is needed and thus being suitable for the telecom industry [11].

Unlike other sources of clean energy, it is widely scalable owing to its modular technology to match

future increase in load. However, solar technology presents challenges in terms of high upfront capital expenditure and high space requirements for deploying the plant [11]. Nigeria has an average solar insolation of 5.75 kWh/sq. m/day with an average daily sunshine of 4 to 7.5 hours. The northern region of Nigeria has a high solar potential with an average insolation as high as 7 kWh/sq. m/day. Solar PV is used in some small-scale rural electrification projects by the State/Federal governments [6]

1.2.2 Wind

Wind is a cost effective source of green energy for grid-connected megawatt (MW) scale deployments. Its adoption for small scale distributed energy generation has been hindered by high regular maintenance costs, low reliability due to the variability of wind speed and investment risks. Wind has been adopted in combination with power alternative technologies such as solar where there is a good potential for operations cost savings [11]. The wind resource in Nigeria varies by region with the extreme north region presenting good wind speeds of 4 to 5.1 m/s, suitable for small scale telecom applications. The southern region has an average wind speed of 1.4 to 3.0 m/s except for the coastal and offshore regions [6].

1.2.3 Biomass

Biomass falls lower in the choice of green technology; however it presents a good opportunity for small scale distributed energy generation. The technology is widely available and has been increasingly adopted, thanks to the innovative uses of biomass options. The adoption/uptake of biomass for telecom application however, presents its own challenges in terms of operational complexity and scalability, supply integration and sustainability [11]. Nigeria has a moderate potential for using biomass as a source of electricity. The Energy Commission of Nigeria has put forth plans to produce bio-fuel (bio-ethanol) from sugarcane and cassava plantations with a potential production of 120-140 million liters every year, at 43.4 million tons of fuel wood consumption annually; However, the use of wood waste (a potential of 1.8 million tons of saw dust generated every year) as biomass input for energy production is relatively low [6].

1.2.4 Fuel cell

Over the years, fuel cell technology has seen various innovations including the fuel types and generation technology. Fuel cells based on hydrogen are most popular and the cleanest due to their 100% burning characteristics. However, their adoption is hindered due to high initial capital expense, availability and supply of hydrogen fuel as well as high replacement cost (almost 25-30% of Capital expenditure) of cells every 5-6 years. On-site hydrogen fuel generation is an alternative option to consider for countries without a reliable fuel supply chain; however the technology and pilot demonstration haven't reached the telecom application in this region; hydrogen fuel supply chain is not yet established in Nigeria [11].

1.2.5 Hydro (Pico)

Hydro power is the most traditional form of clean energy for large scale (megawatt scale), grid-connected power generation and so far, its adoption at small scale distributed generation has been limited due to lack of technology and suppliers. Other challenges for telecom applications include the availability of water body resources, adjacent to or near to the site location. The capital expenditure requirements and potential business case for telecom applications is yet to be known. The potential for Pico-hydro based power alternative for telecom applications is yet to be established for Nigeria [11].

II. Overview of the Review

From the review of these few past works, it is obvious that a lot of research work has been done in the area of powering of Telecom base stations through renewable energy sources, particularly solar power system.

This notwithstanding, this work shall attempt to consolidate on past research work and to also investigate more effective and efficient strategies of deploying solar power at a base transceiver station.

2.1 Why the Choice of Solar Alternative Power

Considering the challenges hindering the deployment of all the highlighted power alternatives above, with respect to the Nigerian environment and with the fact that approximately 56% of potential BTS sites are off-grid and 44% are unreliable grid sites [11], we decided to adopt the solar option; as Nigeria has a high solar potential and solar panels technology is gradually being accepted in the country with majority of the materials required readily available. Also, it is estimated that the implementation of this power alternative for 10,890 potential sites would save around N3.168 billion in operations expenses and reduce diesel consumption by approximately 76% from current levels. The payback period would be around 2.7 years with an initial investment of approximately N78.375 million per site [11]. The estimate is based on sizing of the solar-hybrid power systems for the current load requirements considering an average Diesel Generator running of 4 hours per day [11].

2.2. Solar (PV) panel theory and construction

Based on semi-conductor technology solar cells operate on the principle that electricity will flow between two semi-conductors when they are put into contact with each other and exposed to light (photons). The phenomenon

known as photovoltaic effect was first discovered by Edward Becquerel in 1839 [4]. The majority of modules used wafer-based crystalline silicon cells; these cells must also be protected from mechanical damage and moisture.

Electrical connections are made in series to achieve a desired output voltage or in parallel to provide a desired current capability. The conducting wires that take the current off the modules may contain silver, copper or other non-magnetic conductive transition metals. The cells must be connected electrically to one another and to the rest of the system. Array currents up to 20% greater than the specified output have been reported [9].

In this project work, the Mono-crystalline type of Silicon panel would be utilized because a higher voltage is required and the dc power to be produced has to travel some distance before being utilized or stored in a battery bank. Also, this type of panel is the most efficient PV technology averaging 14% to 17% [9]. The deep cycle type of battery would also be deployed for the battery bank in this project work.

III. DESIGN AND ANALYSIS OF THE SOLAR POWER SYSTEM FOR A TYPICAL GSM BTS

3.1 METHODOLOGY

The main method employed in this research project has been broken down into different functional blocks, to better explain the complete operation of the circuit design. This has been done so, to reduce the complexity involved in designing a pure sine wave or even a rectified circuit; since many steps would be involved in carrying out dc-to-dc, dc-to-ac or even ac-to-dc conversions. The detailed function of each section with the mathematical models of the output voltage (i.e. voltage-time operations) has also been discussed in this chapter.

3.2 DEVELOPMENT OF BLOCK DIAGRAM

Figure 3.1 below shows a description of the present power design used in a typical GSM BTS in Nigeria; while Fig. 2 shows a description of the various parts of this research project as would be implemented. This block diagram shows the arrangement needed to generate the necessary output signals at each output points of the circuit in Fig. 3.

The first part of the block diagram indicates the input voltage source through the Solar Panel; priority is given to the dc voltage (120Vdc) supplied by the Solar Panel even though the Rectifier supplies a dc voltage too after receiving input from the Generator set (i.e. when the Solar Panel is not operating).

The dc voltage output is stepped down as it passed into a Buck converter through a dc fuse board, and an output of 48Vdc is obtained from there to power up the dc load on site. This dc voltage from the Solar Panel is also stepped up to 220Vdc by a Boost Converter and this output is then passed to a dc-to-ac converter, to give an output of 220Vac which is used to power the ac loads on site.

A functional block for the battery charger is also shown, from where the battery bank is being charged as the Solar Panel serves as the source for this circuit and the battery bank the sink. Also, this battery bank serves as the voltage source for this circuit anytime the Solar Panel is not supplying voltage to the circuit as can be seen in the reverse path into the ATS from Fig. 2, thus the Solar Panel serves as the sink in this instance.

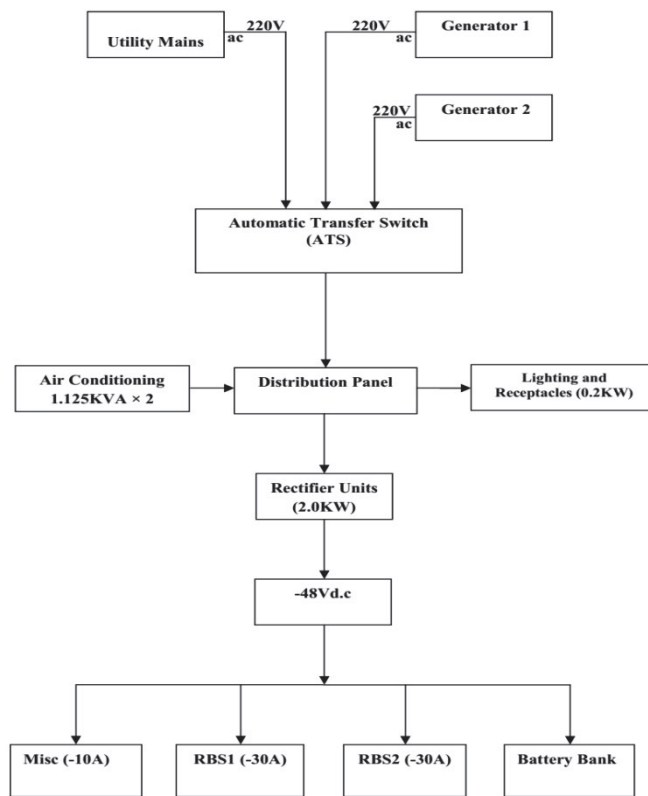


Fig. 1 Present Base Station Power Design

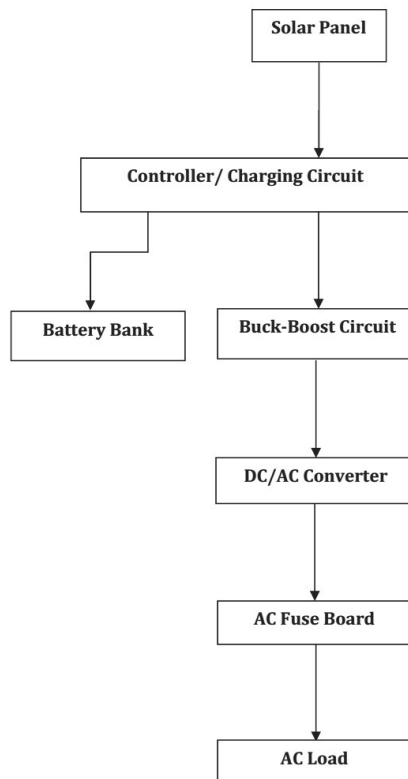


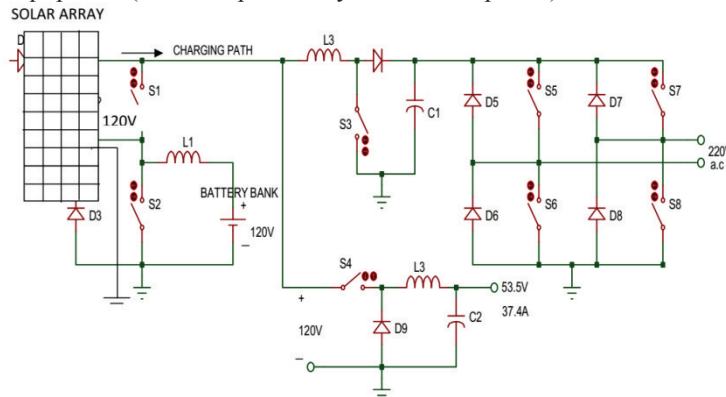
Fig. 2 Block Diagram of Solar Power System for a Typical GSM BTS

3.3 DESIGN PROCESS

This explains the circuitry design process for the research work. When the solar panels receives enough energy from sunlight, the solar photovoltaic (PV Array) become sufficiently charged and voltage is generated then

passed in dc form to the Buck converter. As the Solar array is in its ON state, the battery bank shown in Figure 3.3 (L1 and S2) would be charging while the solar array supplies a voltage of 120Vdc to the Boost converter (L2,D4,C1,S3).

The Boost converter steps up this voltage to 220Vdc and then passes it to the dc-to-ac converter (D5, D6, S5, S6, D7, D8, S7, and S8), which converts the 220Vdc to 220Vac in order to power the ac load (e.g. socket outlets). Also the Buck converter (S4, L3, C2, D9), steps down the 120Vdc from the solar array to 53Vdc for the point-to-point microwave radio equipment (which requires only -48Vdc to operate).



BATTERIES = 12V, 110AH

PANEL = MONOCRYSTALLINE 80WATTS

Fig. 3 Circuit Diagram of Solar Power System for a Typical GSM BTS

3.3.1 Filter circuit design

The filter circuit is an important part of the circuitry design for this work; it consists of an L-C circuit which produces an output with low harmonics, thus making it possible to achieve a well-shaped, pure sine wave output. This circuit is a two-quadrant converter circuit as shown in Fig.4; D1, S1 and D4, S4 form the first quadrant while D2, S3 and D3, S2 form the second quadrant. When S1 and S4 are in the ON state, S2 and S3 remain switched OFF; while the reverse operation occurs for S1 and S4 when S2 and S3 are switched ON (i.e. S1 and S4 would be OFF then). The switching pulses for these two quadrants form square waves at the output of the two-quadrant H-bridge (Full-bridge) inverter shown in Fig. 4 below, while the L-C circuit now reshapes the output into a pure sine wave.

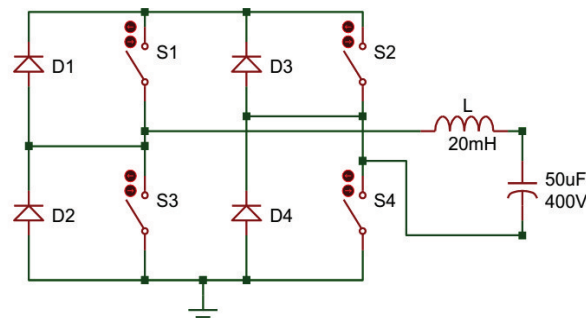


Fig. 4 Filter Circuit Design

3.3.2 Logic circuit for the inverter

This circuit is also very important in the overall working process of this design. As shown in Fig. 5, it consists of an oscillator circuit whose function is to generate the triangular wave and the comparator circuit which shapes the triangular wave into its positive and negative components. There is another oscillator circuit referred to as the sine-wave oscillator circuit, which simply functions as the circuit generating the required sine wave; it is connected directly to another comparator circuit (phase inverter), which helps in negating the phase of the sine wave generated from the sine-wave oscillator circuit.

Finally, there are the dual-comparator circuits with each receiving inputs separately from the triangular wave oscillator and the sine-wave oscillators respectively. The outputs of these comparators form a triangular wave which is enveloped in the inverted sine wave generated by the sine-wave oscillator circuit (i.e. phase inverted sine wave).

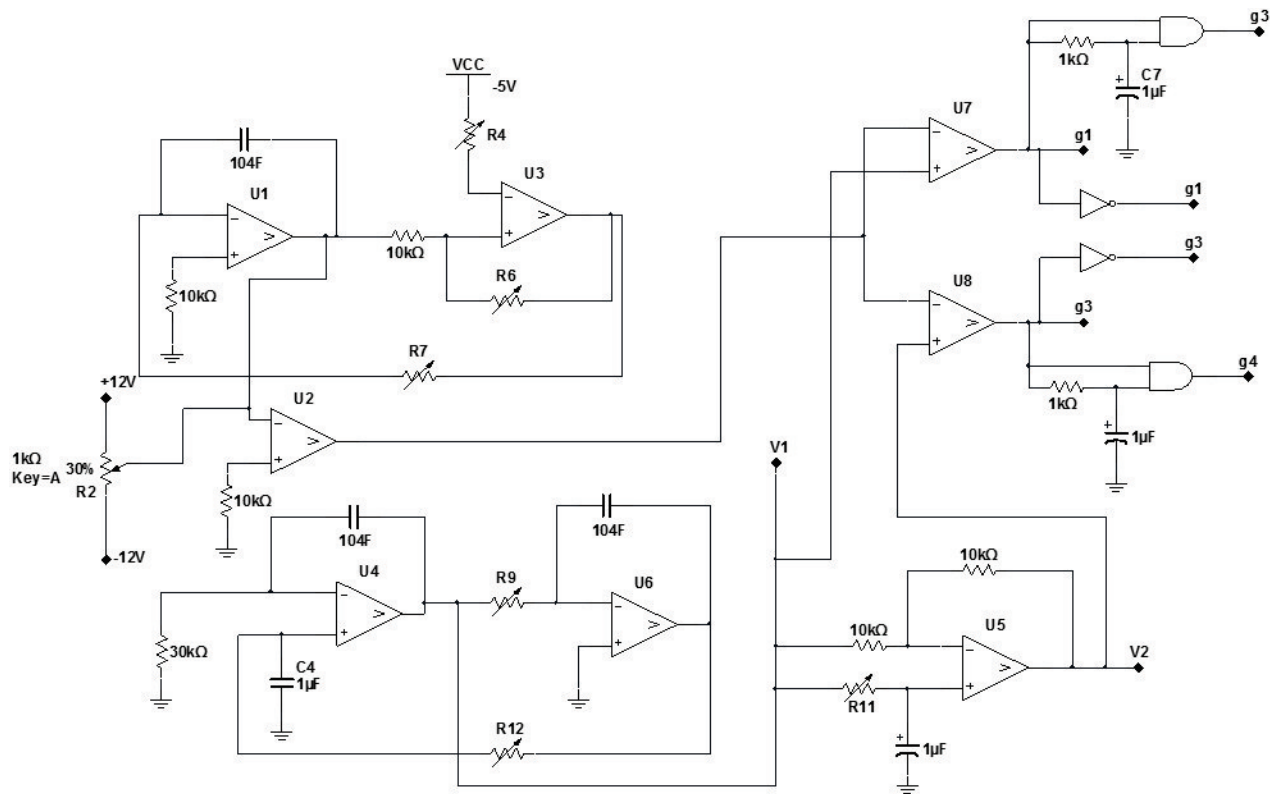


Fig. 5 Logic Circuit for the Inverter Circuit

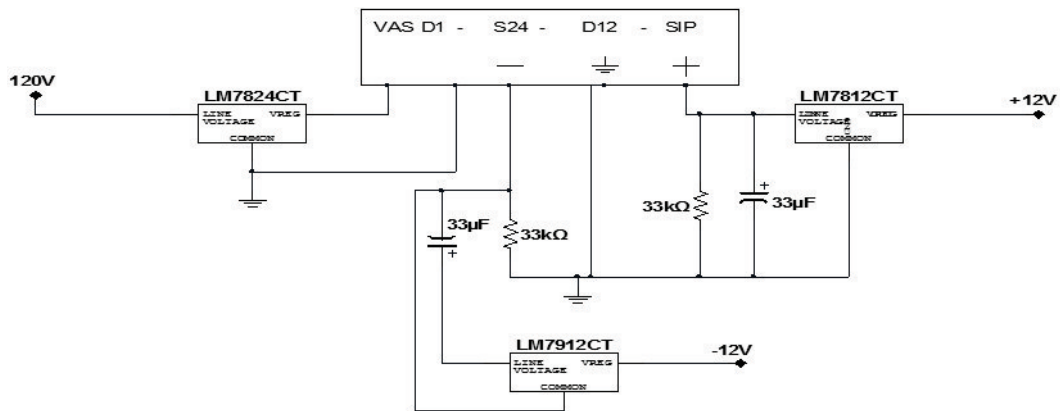


Fig. 6 Power Supply for Isolation Circuit

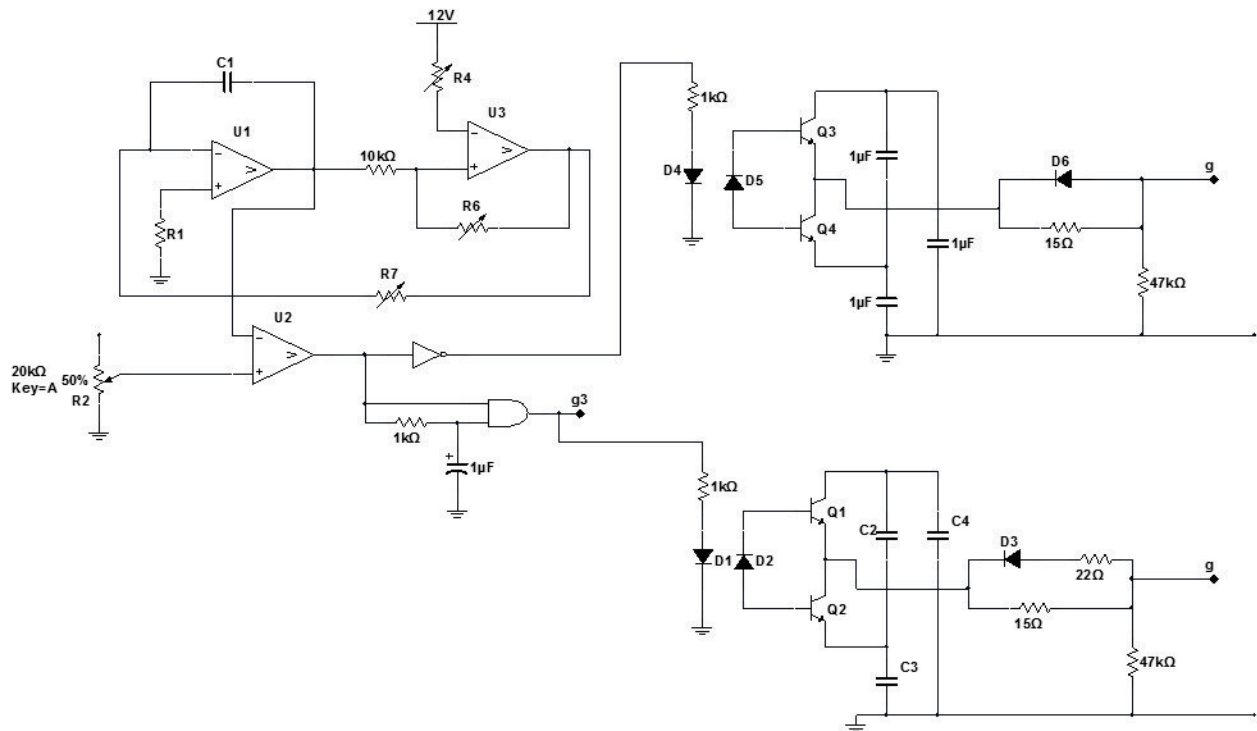


Fig. 7 Gating Signal for the Buck-Boost Circuit

3.3.3 Two-Quadrant D.C-D.C converter

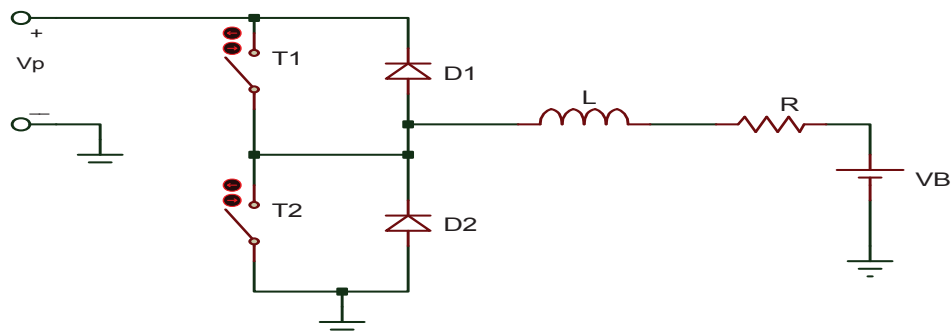


Fig. 8 Two-Quadrant DC-DC Converter

The theoretical/mathematical analysis for the above dc-dc converter is explained as follows:

For $T_1 = \text{ON}, T_2 = \text{OFF}$

$$V_p = Ri_0 + L \frac{di_0}{dt} + V_B \quad (1)$$

At time $t = 0$ (sec) i.e $i_{0(0)} = I_{min}$

$$i_0 = Ae^{-t/\tau} + \frac{V_p - V_B}{R} \quad (2)$$

i.e

$$\frac{V_p - V_B}{R} = i_0 + \frac{L}{R} \frac{di_0}{dt} \quad (3)$$

Where

$$\frac{L}{R} \frac{di_0}{dt} = -Ae^{-t/\tau} \quad (4)$$

$$\frac{V_p - V_B}{R} - (-Ae^{-t/\tau}) = Ae^{-t/\tau} + \frac{V_p - V_B}{R} \quad (5)$$

Since $i_o(0) = I_{min}$ equation (1) becomes

$$I_{min} = A e^{(0)} + \frac{V_p - V_B}{R} \quad (6)$$

$$A = I_{min} - \frac{V_p - V_B}{R} \quad (7)$$

Putting equation (7) for 'A' into equation (2)

$$I_o = \left[I_{min} - \frac{V_p - V_B}{R} \right] e^{-t/\tau} + \frac{V_p - V_B}{R} \quad (8)$$

$$I_o = \frac{V_p - V_B}{R} [1 - e^{-t/\tau}] + I_{min} e^{-t/\tau} \quad (9)$$

From equation (9) the value of i_o increases exponentially from I_{min} to a maximum value of I_{max} at $t = t_{on}$

I_{max} is given as:

$$I_{max} = \frac{V_p - V_B}{R} [1 - e^{-t_{on}/\tau}] + I_{min} e^{-t_{on}/\tau} \quad (10)$$

For the interval $t_{on} \leq t \leq T$, T is switched OFF and T2 is turned ON; for current i_o positive, D2 will conduct to give $V_p = 0$

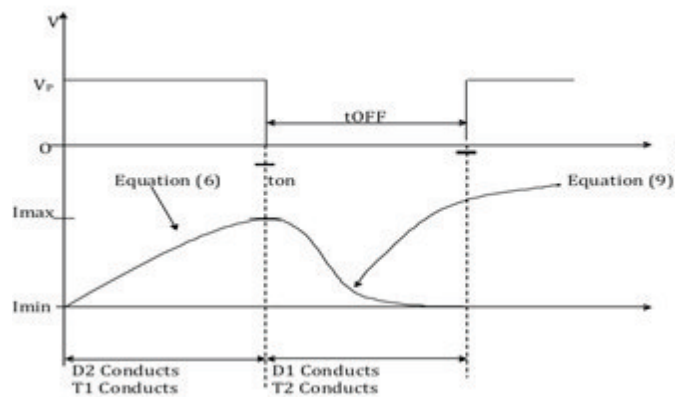


Fig. 9 Two-Quadrant DC-DC Converter Output

Thus, the output equation becomes

$$0 = R i_o + L \frac{di_o}{dt} + V_B \quad (11)$$

At $t_{on} = t$ and $i_o = I_{max}$

Recall that from equation (7)

$$A = I_{min} - \frac{V_p - V_B}{R} \text{ And } V_p = 0$$

$$I_{max} = A_2 - \frac{V_B}{R} \quad (12)$$

Where I_{min} is now I_{max}

$$A_2 = I_{max} + \frac{V_B}{R} \quad (13)$$

$$i_o = \left[I_{max} + \frac{V_B}{R} \right] e^{-\frac{(T-t_{on})}{\tau}} - \frac{V_B}{R} \quad (14)$$

Recalling from equation (2) where

$$i_o = A e^{-t/\tau} + \frac{V_p - V_B}{R} \text{ And } V_p = 0$$

So from equation (14), at $\tilde{t} = T$, the switching period of the current is $I_o = I_{min}$

Therefore,

$$I_{min} = \left(I_{max} + \frac{V_B}{R} \right) e^{-\frac{(T-t_{on})}{\tau}} - \frac{V_B}{R} \quad (15)$$

Solving equation (10) and (15) for I_{min} and I_{max} we get the following:

$$I_{min} = \frac{V_B}{R} \left[\frac{1 - e^{-t_{on}/\tau}}{1 - e^{-T/\tau}} \right] - \frac{V_B}{R} \quad (16)$$

$$I_{max} = \frac{V_B}{R} \left[\frac{1 - e^{-t_{on}/\tau}}{1 - e^{-T/\tau}} \right] - \frac{V_B}{R} \quad (17)$$

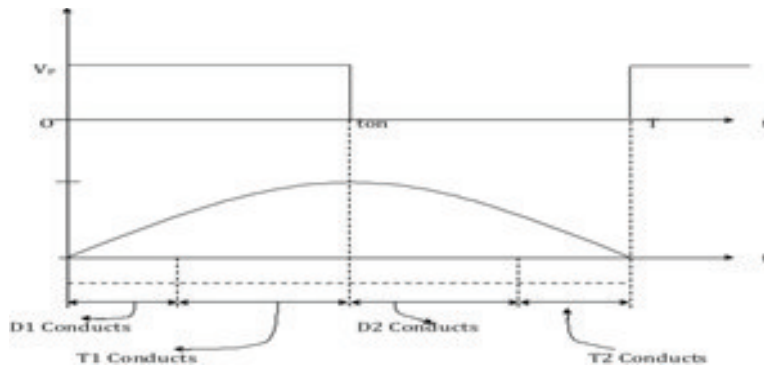


Fig. 10 Negative and Positive Current Flow for T₁, D₁, T₂ and D₂

Note: that the idea of continuous and discontinuous current does not arise, since T₂ and D₁ allows negative current.

Two quadrants here, simply implies that current can either be positive or negative while voltage remains positive. The objective is to conduct a fixed dc to control dc output; therefore, we need to know the average output voltage and current. In addition, we need to know the associated ripples.

The average output voltage V_{oa} is:

$$V_{oa} = \frac{1}{T} \int_0^T V_0 dt \quad (18)$$

$$V_{oa} = \frac{1}{T} \int_0^{t_{on}} V_p dt \quad (19)$$

$$V_{oa} = \frac{t_{on}}{T} V_p \quad (20)$$

The duty cycle $D = \frac{t_{on}}{T}$

Therefore,

$$V_{oa} = DV_p \quad (21)$$

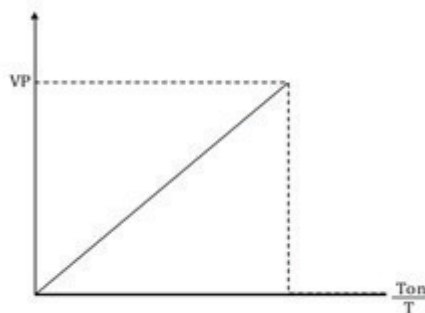


Fig. 11 Plotting Graph of $V_{on} = DV_p$

The graph for equation (21) is given as above in Fig. 11.

3.3.4 The ripple content

There are two approaches to this viz:

- (1) Either $I_{max} - I_{min}$ is kept within a limit or
- (2) The ripple current (Fourier transform) is kept within a maximum tolerable value.

Generally, ripple is reduced to a tolerable value by increasing the inductance L.

In the Fourier form, the output voltage can be expressed as:

$$V_0 = V_{oa} + \sum_{n=1}^{\infty} C_n \sin(n\omega t + \phi_n) \quad (22)$$

Where n is the harmonic order

$$V_0 = DV_p + \sum_{n=1}^{\infty} C_n \sin(n\omega t + \phi_n) \quad (23)$$

Where

$$C_n = \sqrt{a_n^2 + b_n^2} \quad (24)$$

With a_n and b_n defined as:

$$a_n = \frac{1}{T/2} \int_0^{t_{on}} V_0 \cos(n\omega t) dt \quad (25)$$

And

$$b_n = \frac{1}{T/2} \int_0^{t_{on}} V_0 \sin(n\omega t) dt \quad (26)$$

This implies that:

$$a_n = \frac{2}{T} \int_0^{t_{on}} V_p \cos(n\omega t) dt \quad (27)$$

$$a_n = \frac{2V_p}{n\omega T} [\sin(n\omega t)]_0^{t_{on}} \quad (28)$$

Where

$$\omega t = 2\pi$$

$$a_n = \frac{2V_p}{2\pi n} \sin(n\omega t_{on}) = \frac{V_p}{\pi n} \sin(n\omega t_{on}) \quad (29)$$

Similarly

$$b_n = \frac{2}{T} \int_0^{t_{on}} V_p \sin(n\omega t) dt \quad (30)$$

$$b_n = \frac{2V_p}{n\omega T} [\cos(n\omega t)]_0^{t_{on}} \quad (31)$$

$$b_n = \frac{V_p}{\pi n} [1 - \cos(n\omega t_{on})] \quad (32)$$

But,

$$C_n = \sqrt{a_n^2 + b_n^2} \quad (33)$$

$$C_n = \frac{V_p}{\pi n} \sqrt{\sin^2(n\omega t_{on}) + (1 - \cos(n\omega t_{on}))^2} \quad (34)$$

$$C_n = \frac{V_p}{\pi n} \sqrt{2(1 - \cos(n\omega t_{on}))} \quad (34)$$

$$C_n = \frac{V_p \sqrt{2}}{\pi n} [1 - \cos(n\omega t_{on})]^{1/2} \quad (35)$$

The load current is important because, if there are ripples, then definitely there would be losses. The load current is determined from V_{oa} and rms n^{th} harmonic output voltage. The average current I_{oa} is determined from the d.c equivalent output circuit.

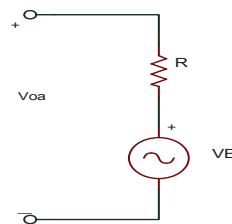


Fig. 12 Average Current Circuit Model

From Fig. 12,

$$I_{oa} = \frac{V_{oa} - V_B}{R} \quad (36)$$

The n^{th} harmonic ripple current is determined from the ac equivalent below:

The n^{th} harmonic rms ripple current is given as

$$I_n = \frac{C_n / \sqrt{2}}{\sqrt{R^2 + (n\omega L)^2}} \quad (37)$$

Rms Load Current is:

$$I_{OR} = \sqrt{(I_0)^2 + \sum_{n=1}^{\infty} (I_n)^2} \quad (38)$$

The ripple content of the load current is:

$$R_{i0} = \frac{\sqrt{\sum_{n=1}^{\infty} I_n^2}}{I_{oa}} \quad (39)$$

R_{i0} should be kept equal to or below 10% (0.1) to reduce harmonic losses.

Alternatively, the Peak-to-Peak ripple current is reduced to a specified percentage of I_{on} .

$$\frac{I_{max} - I_{min}}{I_{o0}} < \text{Specified value}$$

Note: that for this particular consideration ($I_{max} - I_{min}$) maximum occurs at $D = 0.5$

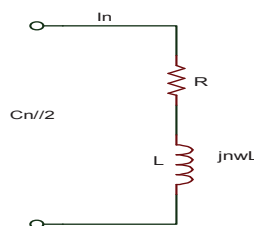


Fig. 13 A.C Equivalent Model

IV. SIMULATIONS AND RESULTS

4.1 EXPERIMENTAL IMPLEMENTATION

The static switched mode power supply together with its control signals which were implemented had a laboratory prototype designed to compare the experimental signal waveforms with the earlier made simulations. The main things considered were the switching voltage and current required to charge the battery bank and power the point-to-point microwave transmission radio.

The circuit diagrams for this implementation are as earlier illustrated in figures 2- 5; the power and driver circuits used are based on the working principle of IGBT driver EXB 841, which provides the power circuit isolation required. The integrated circuit(IC) has a signal isolation circuit which is inbuilt, a driver amplifier, over-current cut-off circuit, over-current detector and gate turn-off power supply. The current sensor LA 55-P/SP1, a closed-loop current transducer was used to measure the line current from the phase in the power circuit. It has a default primary to secondary turn ratio of 1:2000 and for a 30A current measurement, the wire carrying the current was wound round the sensor four(4) times corresponding to a current of 12mA. A resistor of 330 Ω was used to measure the equivalent voltage drop which corresponds to the current passing through the phase.

The ON and OFF switching logic of the power switches for the voltage source inverter is achieved by using the circuit in figure 3.5, from where firing pulses to the inverter switches are generated while a buck converter was built from figure 3.11 to generate switching pulses at 2KHz. The battery charge controller is shown in figure 3.4, it cuts the charging current to the battery at 30A and also cuts the load when the battery voltage is less than 120V.

4.1.1 Experimental results

The laboratory experimental set up and this was done in four stages; Charge-discharge converter for managing the batteries, buck converter to maintain load voltage at 53Vdc and 30A, a boost converter that drives voltage-source and single phase inverter that powers the ac load. The readings from the laboratory setup were taken as displayed on the digital oscilloscope readings in figures 19-23

The waveforms of the buck converter circuit are as depicted in figures 19-21. The switching pulse is generated at a frequency of 5 kHz and duty cycle of 34.2% to drive the power circuit. From fig. 20 and 21, the output voltage was fixed at 53Vdc regardless of the input voltage variation, and all the voltage spikes were filtered at the output. The readings from the laboratory setup were taken as displayed on the digital oscilloscope readings in fig. 19-23

The waveforms of the buck converter circuit are as depicted in fig. 19-21. The switching pulse is generated at a frequency of 5 kHz and duty cycle of 34.2% to drive the power circuit. From fig. 20 and 21, the output voltage was fixed at 53Vdc regardless of the input voltage variation, and all the voltage spikes were filtered at the output.

4.1.2 Computation of the static converter efficiency

The efficiency of the static converter control was computed to approximate the power losses of the charge controllers, buck converter, boost converter and the inverter. The potential difference across the solar array and the array maximum current on full load were measured using the current sensor LA55-P/SP1 which is a closed loop current transducer. It was used to measure the line current from the phases, while the phase voltage was measured as the output of the load.

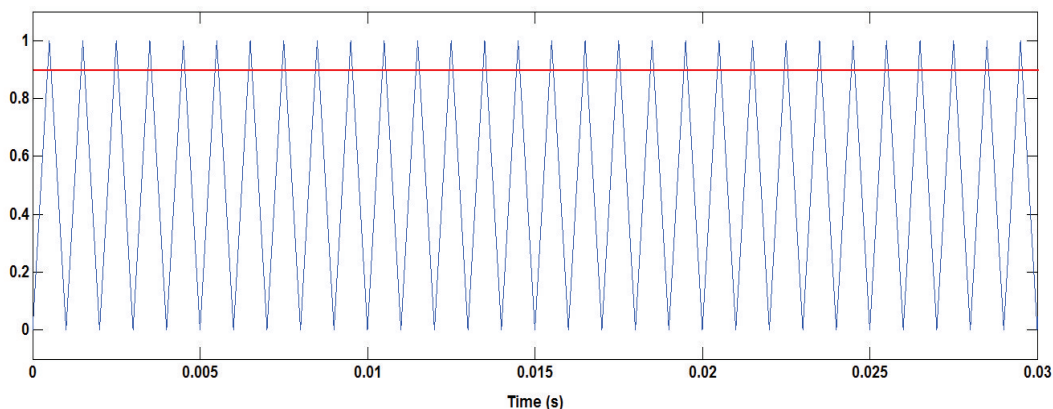


Fig. 14 The Reference Triangular Wave Signal and Battery Feedback Voltage.

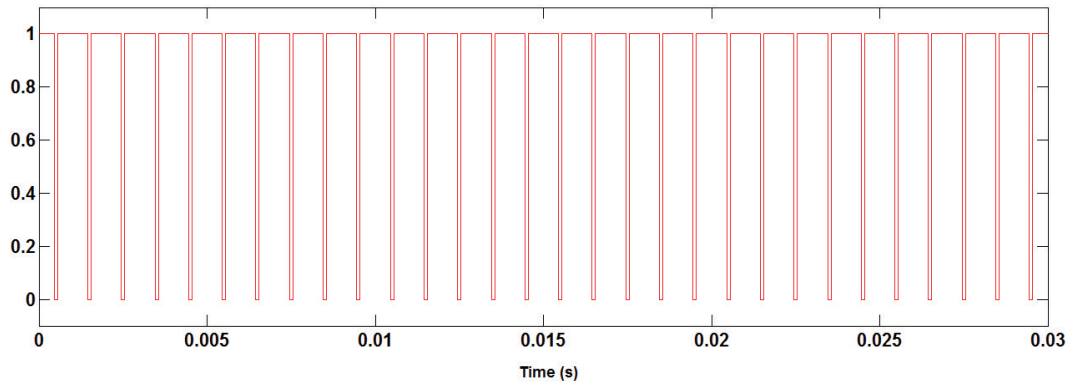


Fig. 15 The Pulse Width Modulation Signals for Charging the Battery.

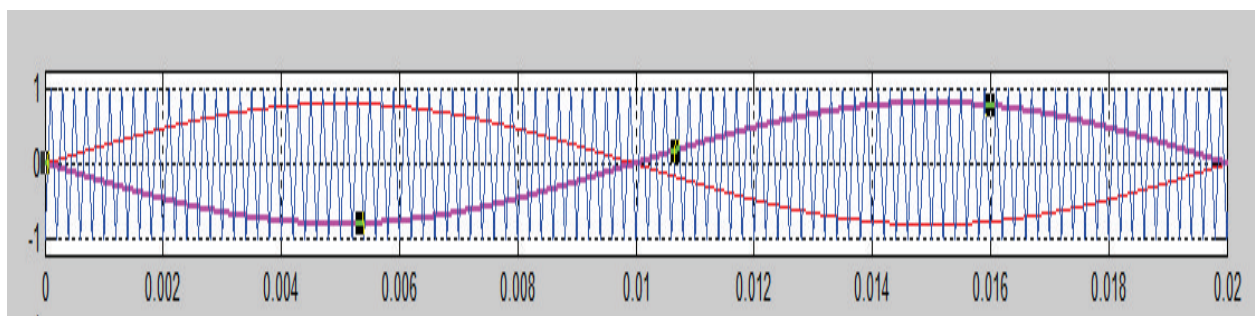


Fig. 16 The Amplitude Modulation (AM) Signal used to Generate the Gating Signals for the H-Bridge Inverter Circuit.



Fig. 17 The Four Modulated Gating Signals for the H-Bridge Inverter

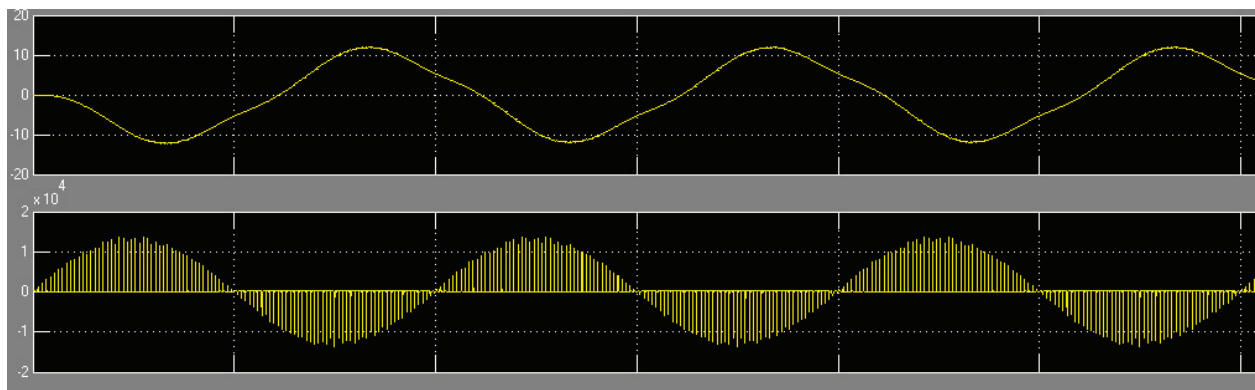


Fig. 18 The Simulated Output Signal of the Inverter

Table 1 Computation of Static Converter Efficiency

S/n	Input			Output			Efficiency(%)
	V _{in} (v)	I _{in} (A)	P _{in} (w)	V _o (v)	I _o (A)	P _o (w)	
1	75.50	21.30	1,608.15	53.1	26.94	1430.51	88.97
2	95.00	16.92	1,607.40	53.1	26.88	1,427.53	88.81
3	115.00	13.97	1,606.55	53.1	26.86	1,426.29	88.78
4	135.00	11.89	1,606.23	53.1	26.84	1,425.21	88.73
5	155.00	10.36	1,606.02	53.1	13.30	1,424.86	88.72
6	175.00	9.18	1,605.91	53.1	15.11	1,424.12	88.68

The following parameters are shown in Table 1:

Input voltage (V_{in}), Input current (I_{in}), Input power (P_{in});
 Output voltage (V_o), Output current (I_o), Output power (P_o).

Also, the input power (P_{in}), Output power (P_o) and Efficiency were calculated using the equation below:

$$Efficiency (\%) = \frac{P_o}{P_{in}} \times 100\% \quad (40)$$

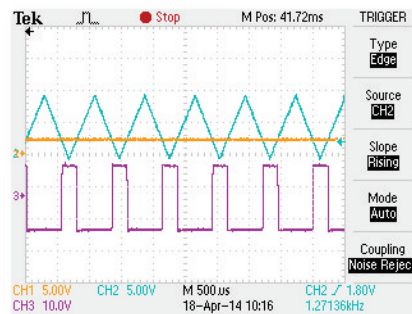


Fig. 19 The Wave Shape of the Switching Pulses at 34.2% Duty-Cycle.



Fig. 20 The Wave Shape of the Load Dc Voltage with an Input Voltage of 175vdc and Output of 53vdc.

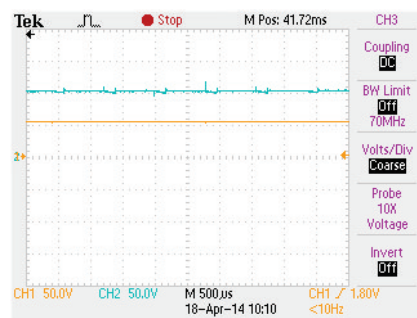


Fig. 21 The Wave Shape of the Load Dc Voltage with an Input Voltage of 95vdc and Output of 53Vdc.

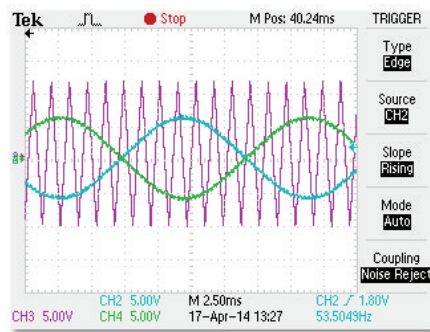


Fig. 22 Waveform of the Sinusoidal Pulse-Width Modulation showing the Carrier and Reference Signals.

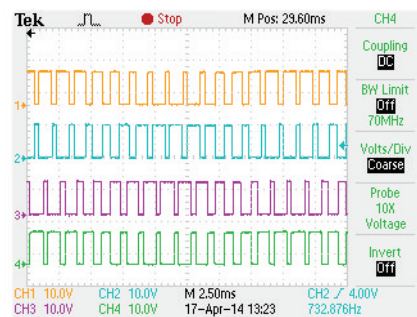


Fig. 23 The Inverted and Non Inverted Firing Pulses for Switching the Upper and Lower Switches of the Inverter

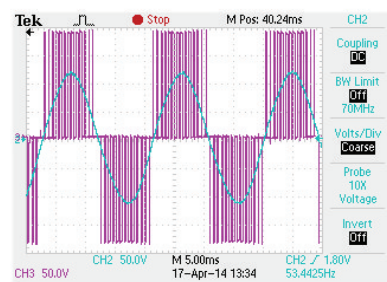


Fig. 24 Pre-Filtering Pure Sine Wave Generated at the Output of the Superimposed-Inverter Output Voltage

V. CONCLUSION

5.1 Discussion

As illustrated in Table 1 (Computation of static converter Efficiency); the average efficiency of the static converter circuit was found to be 88.78%, implying that only an average of 11.22% of the power is lost in the course of power conversion.

The above shows that replacing of the generator sets on site and electricity from mains (PHCN) with Solar PV helps to remove destructive harmonics generated by the rectifier circuits which powers the active devices of the GSM BTS.

Solar PV energy gives a clean output, devoid of surges and power impurities which are harmful to the active BTS devices (e.g. microwave transmission radio equipment). This design allows for sharing of control signals between all the static converters and the inverter, thus increasing efficiency and reliability. This work when implemented will help reduce downtime for telecommunications companies by increasing energy self-sufficiency and securing stable energy sources; while also freeing additional energy for the national grid to power other sectors of the economy. It would also open a window of opportunity for individuals and organizations which have interest in carrying out research for the development of the Nigerian telecommunications sector.

This technology can find use in the powering of rural computer centers, data centers, wireless base stations for schools and offices, ATM machines etc. It can also be useful as a reliable power back-bone for sensitive electronic devices requiring quality power supply.

5.2 Conclusion

Comparisons drawn between the simulated waveforms obtained as shown in fig. 16 to 18 and the waveforms obtained in the actual experimental results of figures 19 to 24 shows that the experimental results obtained

conforms with the theoretical simulated waveforms.

This in conclusion, shows that the aim of this project research has been achieved with respect to the expected outputs at the charge-discharge converter which manages the battery, the buck converter which effectively maintains the load voltage at the desired level (53Vdc), the boost converter which drives the main voltage source and also the single phase inverter which powers the ac load.

REFERENCES

- [1] Alternative and Sustainable Power for Nigerian GSM/Mobile Base Stations, 2012. Infinite Focus Group Publication, Gorey Business Park, Wexford, Ireland.
- [2] Ashok J, Bhaskar, R, Sriram, N, Janani R, and Sneha Raj, 2013. A Qualitative Analysis of Energy Options; Solar PV, Diesel Generators, Batteries and Electrical Grid. Power cellular base stations, Telecom Center of Excellence (RiTCOE) Indian Institute of Technology, Madras.
- [3] British Petrol Statistical Review of World Energy, 2013. www.bp.com/statisticalreview
- [4] Becquerel, A.E, 1839. Photovoltaic Principles, Comt. Rend. Acad. Sci. 9
- [5] Chinnu, P.R, Athulya P. P, 2014. Different methods of modelling PV panels, An overview.
- [6] Energy Commission of Nigeria (ECN), 2014. <http://www.reegle.info/countries/nigeria-energy-profile/NG>,
- [7] Dike, U. I, Anthony, U. A, Ademola, A, 2014. Analysis of Telecom Base Stations Powered By Solar Energy. INTERNATIONAL JOURNAL OF SCIENTIFIC & TECHNOLOGY RESEARCH VOLUME 3, ISSUE 4, ISSN 2277-8616.
- [8] Faruk, N, Ayeni, A.A, Muhammad, M.Y, Olawoyin, L.A, Abubakar, A, Agbakoba, J, Moses, O, 2012. Powering Cell Sites for Mobile Cellular Systems using Solar Power. International Journal of Engineering and Technology Volume 2 No. 5.
- [9] Gabriola, I, 2004. Photovoltaic Design and Installation Manual
- [10] George, J, 2009. Plugging into the Sun
- [11] GSMA Green Power for Mobile, 2013. Powering Telecoms, West Africa Market Analysis Sizing the Potential for Green Telecoms in Nigeria and Ghana.
- [12] Igwue, G, Nentawe, Y.G, Jonathan, A.E, Charles, I.O and Douglas, K, 2014. Research Proposal for Implementing a solar PV-Based Static Converter/Inverter to power an Outdoor Base Transceiver Station (BTS).
- [13] Jaycar Electronics, 2001. Jaycar Electronics Reference Data Sheet (DC-DC Converters)
- [14] Mohan, N, 1989. Power Electronics, Converters, Applications and Design.
- [15] Muhammad Saad Rahman, M.S, 2007. Buck converter design issues.
- [16] Panagiotis, D. D and George, K. K, 2012. On the Design of an Optimal Hybrid Energy System for Base Transceiver Stations. Department of Electrical and Computer Engineering, Aristotle University of Thessaloniki, Thessaloniki, Greece.
- [17] SMA Technical Information, 2013. Telecommunication; Using of Off-Grid inverters SUNNY ISLAND in Base Transceiver Stations.
- [18] State of Digital Media in Nigeria, 2013. Terragon Limited. <http://twinepinenetwork.com/nigeria>.
- [19] Vanguard Newspaper, 2011. <http://www.vanguardngr.com/2011/12/airtel-goes-with-e-site/>
- [20] Vincenzo, M and Alouf, S, 2011. Reducing Costs and Pollution in Cellular Networks, Inria, M.A Sophia. IEEE Communication Magazine.
- [21] Virendra, S, Jaya, D.L, Charhate, S.V, 2015. A Review: Main Aspects of Power Consumption in Wireless Networks. International Journal of Electrical and electronics Engineers ISSN-2321-2055 (E).
- [22] Wissam, B, 2012. Power system considerations for cell tower applications, Technical information from Cummins Power Generation.
- [23] Yinghao Chu, 2011. Review and Comparison of Different Solar Energy Technologies, Global Energy Network Institute (GENI) Publication.

The IISTE is a pioneer in the Open-Access hosting service and academic event management. The aim of the firm is Accelerating Global Knowledge Sharing.

More information about the firm can be found on the homepage:

<http://www.iiste.org>

CALL FOR JOURNAL PAPERS

There are more than 30 peer-reviewed academic journals hosted under the hosting platform.

Prospective authors of journals can find the submission instruction on the following page: <http://www.iiste.org/journals/> All the journals articles are available online to the readers all over the world without financial, legal, or technical barriers other than those inseparable from gaining access to the internet itself. Paper version of the journals is also available upon request of readers and authors.

MORE RESOURCES

Book publication information: <http://www.iiste.org/book/>

Academic conference: <http://www.iiste.org/conference/upcoming-conferences-call-for-paper/>

IISTE Knowledge Sharing Partners

EBSCO, Index Copernicus, Ulrich's Periodicals Directory, JournalTOCS, PKP Open Archives Harvester, Bielefeld Academic Search Engine, Elektronische Zeitschriftenbibliothek EZB, Open J-Gate, OCLC WorldCat, Universe Digital Library, NewJour, Google Scholar

